

Jamming Model for the Extremal Optimization Heuristic

Stefan Boettcher^{1,†} and Michelangelo Grigni^{2,‡}

¹*Physics Department, Emory University, Atlanta, Georgia 30322, USA*

²*Department of Mathematics and Computer Sciences,
Emory University, Atlanta, Georgia 30322, USA*

(Dated: March 9, 2019)

Extremal Optimization, a recently introduced meta-heuristic for hard optimization problems, is analyzed on a simple model of jamming. The model is motivated first by the problem of finding lowest energy configurations for a disordered spin system on a fixed-valence graph. The numerical results for the spin system exhibit the same phenomena found in all earlier studies of extremal optimization, and our analysis of the model reproduces many of these features. PACS number(s): 02.60.Pn, 05.40.-a, 64.60.Cn, 75.10.Nr.

I. INTRODUCTION

Many situations in physics and beyond require the solution of NP-hard optimization problems, for which the typical time need to ascertain the exact solution apparently grows faster than any power of the system size [1]. Examples in the sciences are the determination of ground states for disordered magnets [2, 3, 4, 5] or of optimal arrangements of atoms in a compound [6] or a polymer [7]. With the advent of ever faster computers, the exact study of such problems has become feasible [8, 9]. Yet, with typically exponential complexity of these problems, many questions regarding those systems still are only accessible via approximate, heuristic methods [10]. Heuristics trade off the certainty of an exact result against finding optimal or near-optimal solutions with high probability in polynomial time. Many of these heuristics have been inspired by physical optimization processes, for instance, simulated annealing [11] or genetic algorithms [12].

Extremal optimization (EO) was proposed recently [13], and has been used to treat a variety of combinatorial [14, 15] and physical optimization problems [5]. Comparative studies with simulated annealing [13, 14, 16] and other Metropolis based heuristics [17] have established EO as a successful alternative for the study of NP-hard problems, especially near phase transitions [16] that are associated with the most complex instances of such problems [18, 19, 20, 21].

In this paper, we investigated some properties of the EO algorithm with analytical means. We motivate our theoretical model system with a brief study of a disordered spin system on a random graph. EO applied to finding ground states of this system reveal the same generic properties found for the algorithm in all previous studies. We can abstract a set of evolution equations from this problem, which allow a complete analysis of EO as a function of its single parameter, τ , and the system size, n . In particular, an optimal value for τ as a function of n is determined in close analogy with the scaling found numerically in all previous studies [22]. We finish

with a discussion on how this model can be used also to investigate alternative versions of EO, or to analytically compare EO with simulated annealing and other local search heuristics.

II. SPIN GLASSES ON FIXED-VALENCE RANDOM GRAPHS

Disordered spin systems on random graphs have been investigated as mean-field models of spin glasses [23] or optimization problems [24, 25], since sites are long-range connected yet have a small number of neighbors. Particularly simple are α -valent random graphs [25, 26, 16]. In these graphs each vertex possesses a fixed number α of bonds to randomly selected other vertices. Specifically, we have used the method described in Ref. [27] to generate these graphs which are also referred to as α -regular graphs. (Note that self loops or double connections are not allowed, and disconnected graphs are highly unlikely). Just as on a lattice, one can assign a spin variable $x_i \in \{-1, +1\}$ to each vertex, and couplings $J_{i,j} \in \{-1, +1\}$ to existing bonds between neighboring vertices i and j . The energy of the system then is the difference between violated bonds and satisfied bonds,

$$H = - \sum_{\{bonds\}} J_{i,j} x_i x_j. \quad (1)$$

It is more convenient to consider a linearly related quantity, which merely tallies to number of violated bonds per spin in a configuration,

$$e = \frac{H}{2n} + \frac{\alpha}{4} \geq 0, \quad (2)$$

using the fact that each graph has a total of $\alpha n/2$ bonds.

Clearly, for all $J_{i,j} \equiv 1$ the spin system has two ferromagnetic ground states with $e = 0$ that are easy to find (all $x_i = 1$ or all $x_i = -1$). But for anti-ferromagnetic bonds $J_{i,j} = -1$, the ground state energy depends on the disordered structure of the graph itself. Only if all loops

in the graph were of even length (like in a hyper-cubic lattice), there are again simple ground states, each with an alternating spin pattern (Neél state). Instead, in a random graph, the disorder creates loops that have an equal chance to be odd or even length. Thus, on average, half of the loops can have all bonds satisfied, the other half will have at least one bond frustrated. Since the length of loops in random graphs typically diverges with $\log(n)$, each odd loop almost certainly has other odd loops as a neighbors to share a violated bond with. In fact, even for a spin glass, $J_{i,j} \in \{-1, +1\}$, the same argument should hold, since only half of the loops will be frustrated and neighboring frustrated loops can share violated bonds. We find that the average ground state energies found for either bond distribution are identical for $n \rightarrow \infty$, in support of the above argument, but the results appear to differ in next-to-leading order corrections.

A τ -EO algorithm for α -valent graphs

To obtain the numerical results in Fig. 1, we used the following implementation of τ -EO (see also Ref. [5]): For a given spin configuration on a graph, assign to each spin x_i an “fitness”

$$\lambda_i = -\#\text{violated bonds} = -0, -1, -2, \dots, -\alpha, \quad (3)$$

so that

$$e = -\frac{1}{2n} \sum_i \lambda_i \quad (4)$$

is satisfied. Each spin falls into one of only $\alpha + 1$ possible states. Say, currently there are n_α spins with the worst fitness, $\lambda = -\alpha$, $n_{\alpha-1}$ with $\lambda = -(\alpha - 1)$, and so on up to n_0 spins with the best fitness $\lambda = 0$. (Note that $n = \sum_i n_i$.) Now draw a “rank” k according to the distribution

$$P(k) = \frac{\tau - 1}{1 - n^{1-\tau}} k^{-\tau} \quad (1 \leq k \leq n). \quad (5)$$

Determine $0 \leq j \leq \alpha$ such that $\sum_{i=j+1}^{\alpha} n_i < k \leq \sum_{i=j}^{\alpha} n_i$. Finally, select any one of the n_j spins in state j and reverse its spin *unconditionally*. As a result, it and its neighboring spins change their fitness. After all the effected λ 's and n 's are reevaluated, the next spin is chosen for an update.

This EO implementation updates spins with a (τ -dependent) bias against poorly adapted spins due to Eq. (5). This process is “extremal” in the sense that it focuses on atypical variables, and it forms the basis of the EO method. The only adjustable parameter in this algorithm is the power-law exponent τ . For $\tau = 0$, randomly selected spins get forced to update, resulting in merely a random walk through the configuration space. The search is ergodic but yields poor results. For $\tau \rightarrow \infty$,

only spins in the worst state get updated which quickly traps the update process to a small region of the configuration space which may be far from a near-optimal solution. Ergodicity is broken in the sense that configurations far from the initial conditions are unlikely to be reached within a given runtime. The dependence of performance on τ for this and all previous implementations of τ -EO (for quite different optimization problems [22, 5]) exhibits the features shown in Fig. 2: The best average performance in approximating ground state energies at a fixed runtime is obtained for a value of τ_{opt} slightly larger than 1, and $\tau_{\text{opt}} \rightarrow 1^+$ for $n \rightarrow \infty$. In fact, the (more extensive) numerical data presented in Ref. [22] suggested

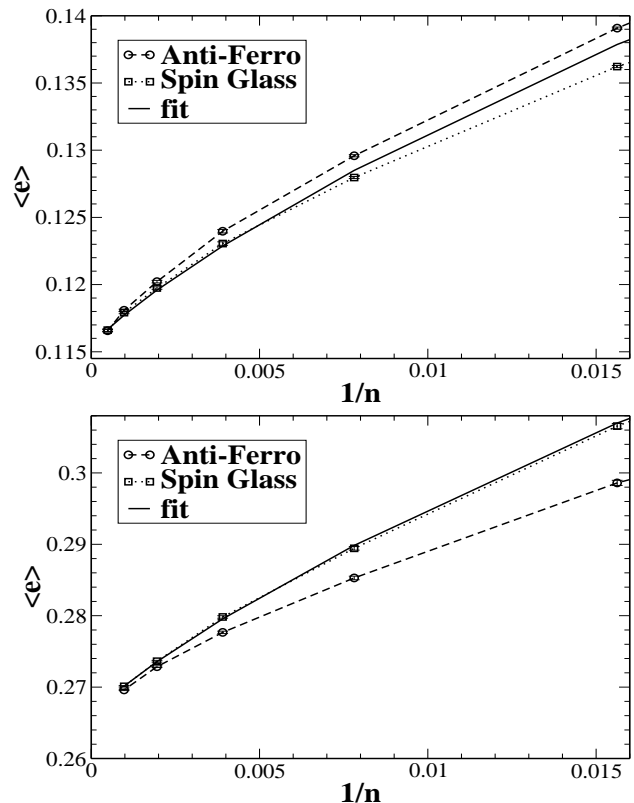


FIG. 1: Extrapolation for the number of violated bonds per spin, e , as a function of $1/n$ (a) for trivalent and (b) for 4-valent graphs of size $n = 32, 64, \dots, 1024$. Circles refer to an anti-ferromagnetic, and the squares to a $\pm J$ bond distribution. The error bars for $\langle e \rangle$ are smaller than the symbols. The data for the spin glass is independent of the way the α -valent graph was formed and is best fit (continuous line) by $e_{\alpha=3}(\infty) = 0.1155(5) + 0.35 \ln(n)/n$ and $e_{\alpha=4}(\infty) = 0.266(1) + 0.63 \ln(n)/n$. We found that the data for the anti-ferromagnet for smaller n varies strongly with the way the α -valent graph was formed (here we used the method described in Ref. [27]) and is difficult to fit. It is apparent, though, that the difference between the data for the spin glass and the anti-ferromagnet is decreasing for $n \rightarrow \infty$.

a simple argument that yields

$$\tau_{\text{opt}} \sim 1 + \frac{\ln\left(\frac{a}{\ln n}\right)}{\ln n}, \quad (n \rightarrow \infty, \ln(n) \ll a \ll n), \quad (6)$$

where $t_{\text{max}} = a \times n$ was used as the maximum number of updates for a single EO run. This asymptotic behavior was justified by placing τ_{opt} at the “edge to ergodicity,” a point between having τ large enough to descent into local minima while having τ just small enough to not get trapped inside the basin of local minima. In the following we present a model to make this notion concrete.

III. EVOLUTION MODELS

We can abstract the random glass problem in Sec. II into a simple model which demonstrates previous observations about τ -EO in an analytically tractable way. Consider the spin system on an α -valent graph. Each spin i can be in one of $\alpha + 1$ states λ_i : either no adjacent bond is violated and i is among the n_0 spins, only one bond is violated placing it among the n_1 spins, and so forth up to the n_α spins which have all their adjacent bonds violated. Thus, one can define densities for each of the $\alpha + 1$ states, $\rho_i = n_i/n$ ($i = 0, \dots, \alpha$). In general, we can interpret any local search procedure, which only updates a single variable at a time, simply as a set of

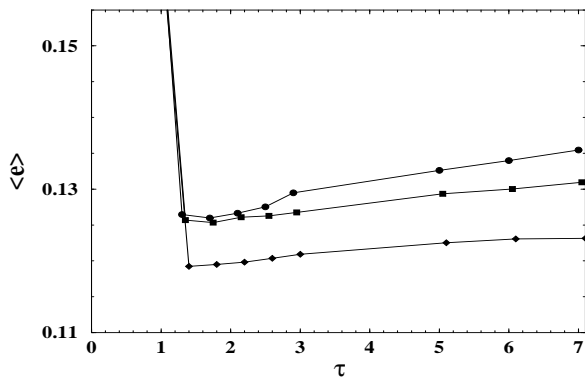


FIG. 2: Plot of the number of violated bonds per spin $\langle e \rangle$ as a function of τ as obtained by τ -EO for a $\pm J$ -spin glass on trivalent graphs. Shown are the results for e averaged over 4 runs each on a set of 20 graphs for $n = 128, 256$, and 512 . While the results clearly get worse rapidly for $\tau < 1$, even for larger τ a decline in the quality can be observed. (The weak dependence of e for large τ may indicate that a greedy approach to finding ground states will yield good approximations [25].) Despite of the slow variation with τ , the value of τ_{opt} where $\langle e \rangle$ is minimized clearly decreases toward $\tau = 1$ with increasing n , consistent with Eq. (6).

evolution equations for the $\rho_i(t)$, to wit

$$\dot{\rho}_i = \sum_j T_{i,j} Q_j. \quad (7)$$

Here Q_j is the probability that a spin in state j gets updated, and the matrix $T_{i,j}$ specifies the net transition to state i given that a spin in state j is updated. Note that conservation of probability requires

$$\sum_j Q_j = 1, \quad (8)$$

and conservation of variables requires

$$\sum_i T_{i,j} = 0 \quad (0 \leq j \leq \alpha). \quad (9)$$

Both, \mathbf{T} and \mathbf{Q} may generally depend on the $\rho_i(t)$ as well as on t explicitly. (For instance, for simulated annealing with a temperature schedule, the Q_i could depend explicitly on t through the changing temperature.)

Another relation is provided by the constraint

$$\sum_i \rho_i(t) = 1, \quad (10)$$

which implies $\sum_i \dot{\rho}_i = 0$. Thus, one of the equations in (7) is always redundant. The cost per variable to be minimized in Eq. (2) now reads

$$e = \frac{1}{2} \sum_i i \rho_i \geq 0, \quad (11)$$

with $e = 0$ being optimal.

The advantage of this notation lies in the fact that the average update *preference*, \mathbf{Q} , is separate from the update *process* described by \mathbf{T} . For instance, for a random walk (equivalent to τ -EO at $\tau = 0$ or simulated annealing at high temperature) $Q_j(t) \equiv \rho_j(t)$, since the probability that a spin in state i gets chosen for an update is equal to the number of those spins, no matter how that update is processed by \mathbf{T} . What is typically unknown for a hard problem is the general form of \mathbf{T} . But to understand the properties of a heuristic expressed in \mathbf{Q} , it may be revealing to “design” interesting \mathbf{T} .

A Annealed approximation to the glass problem

We can construct \mathbf{T} for the glass problem in Sec. II on a trivalent graph in an annealed approximation. Since \mathbf{T} in this case is quite messy, and of no great consequence beyond this Section, we focus on one of its components, say, $T_{1,2}$. This component represents the net flux in or out of ρ_1 , given that a variable in state 2 gets updated. The annealed approximation consists of the unbiased assumption that each of the $\alpha = 3$ neighboring vertices can be in state i with probability ρ_i independently. Of

course, no neighboring vertex can be in state 0, if the bond to it is violated, or in state α , if the bond is good.

For $T_{1,2}$, the vertex chosen for an update has 2 violated bonds and $\alpha - 2 = 1$ good bond. First, when that vertex flips, there is a shift of one variable (fraction $1/n$) from ρ_2 to ρ_1 . The neighboring vertex on the other end of each of the violated bonds could be in state 1, 2, or 3 with probability ρ_1 , ρ_2 , or ρ_3 , respectively, and the vertex attached via the good bond could be in state 0, 1, or 2 with probability ρ_0 , ρ_1 , or ρ_2 , respectively. Considering all allowed combinations, we can find the relative (unnormalized) influx into any of the ρ_i as a consequence of updating the vertex at the center. The sum of the influxes should equal the fraction of moved vertices, α/n , and the relative influxes can be normalized accordingly. Finally, one can identify for each of the combinations where that fraction of moved vertices originated from, which leads to negative out-flux to the $T_{i,2}$ [which is obviously required to satisfy Eq. (9)]. The out-flux out of state i must be proportional to ρ_i . Thus, we obtain the following three terms contributing to $T_{1,2}$:

$$T_{1,2} = \frac{1}{n} + \frac{\rho_0 \rho_1 + 2 \rho_1 \rho_2 + \rho_0 \rho_3 + 2 \rho_2^2 + 3 \rho_0 \rho_2}{n(1 - \rho_0)(1 - \rho_3)} - \frac{(3 \rho_1 + 3 \rho_2 + \rho_3 + 2 \rho_0) \rho_1}{n(1 - \rho_0)(1 - \rho_3)}, \quad (12)$$

and the construction of the other elements of \mathbf{T} in this annealed approximation proceeds equivalently.

It is not too hard to obtain some steady state ($\dot{\rho} = 0$) results for Eqs. (7) with this particular \mathbf{T} , supplemented by Eq. (10). One example would be the random walk limit, $Q_i = \rho_i$, equivalent to $\tau = 0$. More revealing for the analysis of EO is the $\tau \rightarrow \infty$ limit. In that case, on each update only one among the worst spins gets flipped. From some random initial conditions, EO would empty out state 3 first ($Q_3 = 1$, $Q_{2,1,0} = 0$), then empty out 2, and so on, until a steady state is reached with the highest non-empty state being ρ_j with some $j > 0$. In this steady state, we can try to determine the $\rho_i(\infty)$ with the ansatz $Q_i = c_i$, $\sum_i c_i = 1$, where the average is taken over time. The only consistent balance is obtained with state 3 totally empty, $\rho_3(\infty) = 0$ and $c_3 = 0$, and state 2 almost empty except for a single spin reaching the state sometimes, i. e. $\rho_2(\infty) \approx 0$ and $c_2 > 0$. Hence, $c_0 = 1 - c_1 - c_2$ and $\rho_1 = 1 - \rho_0$, which leads to a drastically simplified equations:

$$\begin{aligned} 0 &= c_2(3 + 2\rho_0) + c_1(2 + \rho_0) - (1 + 3\rho_0), \\ 0 &= c_2(1 - 4\rho_0) - c_1(1 + 2\rho_0) - (3 - 6\rho_0), \\ 0 &= -c_2(3 - 2\rho_0) + c_1\rho_0 + 3(1 - \rho_0), \end{aligned} \quad (13)$$

all other equations being redundant. The solution is

$$\begin{aligned} \rho_0(\infty) &= 1, \quad \rho_1(\infty) = 0, \\ c_1 &= \frac{1}{2}, \quad c_2 = \frac{1}{2}, \end{aligned} \quad (14)$$

consistent with numerical simulation for all initial conditions. Thus, in the steady state, almost all variables are in the ground state except for a single vertex that is being bounced between state 1 and 2.

The result that EO converges to the ground state for $\tau = \infty$, while reassuring, is not very helpful to understand either EO or the original problem. The annealed approximation has eliminated everything that made the problem interesting, and EO's convergence for $\tau = \infty$ to a perfectly optimized ground state clearly does not resemble our numerical results from Sec. II.

B Models with very simple flows

Our naive annealed approximation has eliminated most of the relevant features of the original, hard problem. Not surprisingly, it also fails to predict the existence of a finite value for τ_{opt} (see Fig. 2); it is easy to convince oneself that $\tau = \infty$ is in fact the best case scenario for τ -EO for all initial conditions and even at finite runtime. Yet, two basic features of the evolution equations remain appealing: (1) The behavior of a system with a large number of variables can be abstracted into a relatively simple set of equations, describing their dynamics with a small set of unknowns, and (2) the separation of update process, \mathbf{T} , and update preference, \mathbf{Q} , lends itself to an analytical comparison between different heuristics. This distinction is possible, of course, only as long as these heuristics can utilize the same single-variable, local search process in \mathbf{T} . The question is: Can we construct interesting processes \mathbf{T} in the sense that they capture salient features observed for local search on real, NP-hard problems? We will show that even the most basic versions of \mathbf{T} provide some insights into the workings of various local search heuristics.

For simplicity, we choose α as small as possible for the three following model situations. Without restriction of generality, in these cases $\alpha = 2$ is sufficient, but more complicated phenomena could be accommodated with more states. First, we consider the most trivial case where a variable when updated merely moves from state i to state $i - 1$ for $i > 0$, or from state 0 to state α (to make every state accessible), $T_{i,j} = [-\delta_{i,j} + \delta_{i,(\alpha+j \bmod \alpha+1)}]/n$. This process is conveniently depicted as a flow chart in Fig. 3a. Clearly, any gradient descent method will be able to reach the ground state $e = 0$ for this process, since there are no barriers. For instance, simulated annealing with zero temperature will reach this state in $O(n)$ trials, and τ -EO for $\tau = \infty$ will reach $e = 0$ in $< n$ steps, when averaged over initial conditions. [Note that in the above notation, $c_i = 1/4$ solves the steady state equations where $c_0 > 0$ implies $\rho_0(\infty) = 1$, $\rho_{i>0}(\infty) = 0$.] Again, $\tau_{\text{opt}} = \infty$ is obvious. In fact, this model can be solved readily for any τ with the methods to be developed

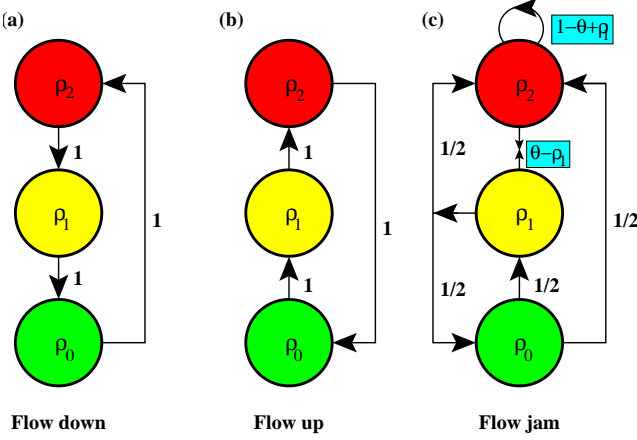


FIG. 3: Plot of the flow diagrams for the different models discussed in the text. Diagram (a) shows a situation in which variables in higher states always evolve toward lower states (except for the lowest state flowing up). In diagram (b), variables have to jump to higher energetic states first before they can attain the lowest state. Diagram (c) shows the model of a jam, where variables in the highest state can only traverse through the intermediate state to the lowest state, if the intermediate state moves its variables out of the way first to keep its density ρ_1 below the threshold θ . The states have energies that increase from the bottom up, the ρ 's mark the occupation density of each state, and arrows out of a state indicate the rates $n T_{i,j}$ at which a variable flows from state j into another state i , if a variable in state j gets updated.

below in Sec. III C. For the random walk limit, $\tau = 0$, it is $c_i = \rho_i(\infty) = 1/4$ since $Q_i \equiv \rho_i$.

Next, we can reverse the directions of transitions in the previous example to obtain a less trivial case, which now possesses energetic barriers. Here $T_{i,j} = [-\delta_{i,j} + \delta_{(\alpha+i \bmod \alpha+1),j}]/n$, as depicted in Fig. 3b. Remarkably, the previous analysis for τ -EO (at least, for $\tau = 0$ or ∞) does not change. The $e = 0$ steady state is reached again in $< n$ steps for $\tau = \infty$, since EO does not reject uphill moves which are required here to arrive at state 0 through state 3, and $\tau_{\text{opt}} = \infty$ again. On the other hand, it is quite clear that simulated annealing will not arrive at $e = 0$ with finite probability in polynomial time, even for a sophisticated temperature schedule. Such energetic barriers are an inherent feature of many NP-hard problems, which makes this simple model quite revealing.

C Model with jammed flow

Naturally, the range of phenomena found in a local search of NP-hard problems is not limited to energetic barriers. After all, so far we have only considered con-

stant entries for $T_{i,j}$. Therefore, in our next model we want to consider the most simple case of \mathbf{T} depending linearly on the ρ_i 's. Most of these cases reduce to the phenomena already discussed in the previous examples. A entirely new effect arises in the following case, also depicted in Fig. 3c:

$$\begin{aligned}\dot{\rho}_0 &= \frac{1}{n} \left[-Q_0 + \frac{1}{2}Q_1 \right], \\ \dot{\rho}_1 &= \frac{1}{n} \left[\frac{1}{2}Q_0 - Q_1 + (\theta - \rho_1)Q_2 \right], \\ \dot{\rho}_2 &= \frac{1}{n} \left[\frac{1}{2}Q_0 + \frac{1}{2}Q_1 - (\theta - \rho_1)Q_2 \right], \\ 1 &= \rho_0 + \rho_1 + \rho_2.\end{aligned}\tag{15}$$

Aside from the dependence of \mathbf{T} on ρ_1 , we have also introduced the threshold parameter θ . In fact, if $\theta \geq 1$, the model behaves effectively like the previous models, and for $\theta \leq 0$ there can be no flow from state 2 to the lower states at all. The interesting regime is the case $0 < \theta < 1$, where further flow from state 2 into state 1 can be blocked for increasing ρ_1 , providing a negative feed-back to the system. In effect, the model is capable of exhibiting a “jam” as observed in many models of glassy dynamics [28, 29, 30], and which is certainly an aspect of local search processes.

We proceed to calculate the unique fix point of the system for EO with arbitrary τ . In the general case, the Q 's depend on the ρ 's in a more complicated way. As described in the numerical simulation of the glass on a random graph in Sec. II, each update a spin is selected based on its rank according to the probability distribution in Eq. (5). When a rank $k (\leq n)$ has been chosen, a spin is randomly picked from state α , if $k/n \leq \rho_\alpha$, from state $\alpha - 1$, if $\rho_\alpha < k/n \leq \rho_\alpha + \rho_{\alpha-1}$, and so on. We introduce a new, continuous variable $x = k/n$, approximate sums by integrals, and rewrite $P(k)$ in Eq. (5) as

$$p(x) = \frac{\tau - 1}{n^{\tau-1} - 1} x^{-\tau} \quad \left(\frac{1}{n} \leq x \leq 1 \right), \tag{16}$$

where the maintenance of the low- x cut-off at $1/n$ will turn out to be crucial. Now, the average likelihood that a spin in a given state is updated is given by

$$\begin{aligned}Q_\alpha &= \int_{1/n}^{\rho_\alpha} p(x) dx = \frac{1}{1 - n^{\tau-1}} (\rho_\alpha^{1-\tau} - n^{\tau-1}), \\ Q_{\alpha-1} &= \int_{\rho_\alpha}^{\rho_\alpha + \rho_{\alpha-1}} p(x) dx \\ &= \frac{1}{1 - n^{\tau-1}} [(\rho_{\alpha-1} + \rho_\alpha)^{1-\tau} - \rho_\alpha^{1-\tau}], \\ &\dots \\ Q_0 &= \int_{1-\rho_0}^1 p(x) dx = \frac{1}{1 - n^{\tau-1}} [1 - (1 - \rho_0)^{1-\tau}],\end{aligned}\tag{17}$$

where in the last line the norm $\sum_i \rho_i = 1$ was used. These values of the Q 's completely describe the update preferences for τ -EO at arbitrary τ .

Inserting the set of Eqs. (18) for $\alpha = 2$ into the model in Eqs. (15), we obtain

$$\begin{aligned}\dot{\rho}_0 &= \frac{1}{n(1-n^{\tau-1})} \left[-1 + \frac{3}{2}(1-\rho_0)^{1-\tau} - \frac{1}{2}\rho_2^{1-\tau} \right], \\ \dot{\rho}_1 &= \frac{1}{n(1-n^{\tau-1})} \left[\frac{1}{2} - \frac{3}{2}(1-\rho_0)^{1-\tau} \right. \\ &\quad \left. + \rho_2^{1-\tau} + (\theta - \rho_1)(\rho_2^{1-\tau} - n^{\tau-1}) \right], \\ \dot{\rho}_2 &= \frac{1}{n(1-n^{\tau-1})} \\ &\quad \left[\frac{1}{2} - \frac{1}{2}\rho_2^{1-\tau} - (\theta - \rho_1)(\rho_2^{1-\tau} - n^{\tau-1}) \right], \\ 1 &= \rho_0 + \rho_1 + \rho_2.\end{aligned}\quad (18)$$

We set $A = (1 - \rho_0)^{1-\tau}$ and $B = \rho_2^{1-\tau}$ to obtain for the steady state, $\dot{\rho} = 0$:

$$\begin{aligned}0 &= -1 + \frac{3}{2}A - \frac{1}{2}B, \\ 0 &= \frac{1}{2} - \frac{3}{2}A + B + (\theta - \rho_1)(B - n^{\tau-1}), \\ 0 &= \frac{1}{2} - \frac{1}{2}B - (\theta - \rho_1)(B - n^{\tau-1}), \\ \rho_1 &= A^{1/(1-\tau)} - B^{1/(1-\tau)}.\end{aligned}\quad (19)$$

One of the first three equations is redundant, and we obtain

$$0 = \frac{3}{2}(A - 1) + \left[\theta - A^{1/(1-\tau)} + (3A - 2)^{1/(1-\tau)} \right] (3A - 2 - n^{\tau-1}), \quad (20)$$

where

$$\begin{aligned}\rho_0 &= 1 - A^{1/(1-\tau)}, \\ \rho_2 &= (3A - 2)^{1/(1-\tau)}, \\ \rho_1 &= 1 - \rho_0 - \rho_2.\end{aligned}\quad (21)$$

The implicit Eq. (20) has some remarkable properties. It has a single physical solution for the ρ 's for all $0 \leq \tau \leq \infty$, $0 < \theta < 1$ [31], and all n . In particular, in the thermodynamic limit $n \rightarrow \infty$ a critical point at $\tau = 1$ emerges. If $\tau < 1$, the n -dependent term in Eq. (20) vanishes, allowing A , and hence the ρ 's, to take on finite values, i. e. $e > 0$. If $\tau > 1$, the n -dependent term diverges, forcing A to diverge in kind, resulting in $\rho_0 \rightarrow 1$ and $\rho_i \rightarrow 0$ for $i > 0$, i. e. $e \rightarrow 0$. This behavior of $e(\tau)$ for various n is shown in Fig. 4.

Having a unique fixed point solution seems to be the last word on this problem, with $\tau = \infty$ again being the most favorable value at which the minimal energy $e = 0$ is reached for sure. But it can be shown that the system has an ever harder time to reach that point, requiring typically $t = O(n^\tau)$ update steps for a finite set of initial conditions. Thus, for a given finite computational time

t_{\max} the best results are obtained at some finite value of τ_{opt} . In that, this model provides a new feature — slow variables impeding the dynamics of faster ones [32] — resembling the observed behavior for EO on real problems, e. g. the effect shown in Fig. 2. In particular, this model provides an analytically tractable picture for the relation between the value of τ_{opt} and the effective loss of ergodicity in the search conjectured in Refs. [13, 22].

The generic evolution of the jamming model for $\tau > 1$ is as follows: If the initial conditions place a fraction $\rho_0 > 1 - \theta$ already into the lowest state, most likely no jam will emerge, since $\rho_1(t) < \theta$ for all times, and the ground state is reached in $< n$ steps. But if initially $\rho_1 + \rho_2 > \theta$, and τ is sufficiently larger than unity, EO will drive the system to a situation where $\rho_1 \approx \theta$ by transferring variables from ρ_2 to ρ_1 . Then, further evolution becomes extremely slow, delayed by the τ -dependent, small probability that a variable in state 1 is updated ahead of all variables in state 2. This situation is depicted in Fig. 5.

Clearly, the jam is *not* a steady state solution of the evolution equations in (18). [It is not even a meta-stable solution since there are no energetic barriers. For instance, simulated annealing at zero temperature would easily find the solution in $t = O(n)$ without experiencing a jam. In reality, a hard problem would most certainly contain combinations of jams, barriers, and possibly other features.] But Fig. 5 suggest the right asymptotic approach to evaluate the long-time behavior of the jam: Consider that we start with initial conditions leading to a jam, $\rho_1(0) + \rho_2(0) > \theta$. We can assume that

$$\rho_1(t) = \theta - \epsilon(t) \quad (22)$$

with $\epsilon \ll 1$ for $t \lesssim t_{\text{jam}}$, where t_{jam} is the time at which ϵ gets small. To determine t_{jam} , we apply Eq. (22) to

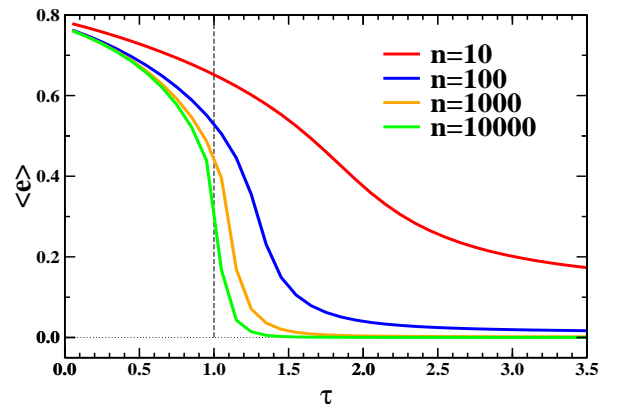


FIG. 4: Plot of $e = \sum_i i \rho_i / 2$ as a function of τ resulting from the solution of Eqs. (20,21) for $\theta = 1/2$ and various values of n . For $n \rightarrow \infty$, a sharp transition emerges at $\tau = 1$, giving optimal results $e \rightarrow 0$ for all $\tau > 1$. But for $\tau > 1$ this steady state is reached only for suitable initial conditions, or after sufficient time, see Fig. 6.

the evolution equations in (18) to get

$$\begin{aligned}\dot{\rho}_0 &\sim \frac{1}{n^\tau} \left[1 - \frac{3}{2}(1 - \rho_0)^{1-\tau} + \frac{1}{2}\rho_2^{1-\tau} \right], \\ 0 &= \frac{1}{2} - \frac{3}{2}(1 - \rho_0)^{1-\tau} + \rho_2^{1-\tau} - \epsilon n^{\tau-1}, \\ 1 &= \rho_0 + \theta + \rho_2.\end{aligned}\quad (23)$$

Here, we have already dropped one of the equations (for $\dot{\rho}_2$) which was redundant. Now, we also can disregard the equation containing ϵ , its importance being that it determines the first-order correction, $\epsilon = O(n^{1-\tau})$, consistently as a function of the leading order contributions of $\rho_0(t)$ and $\rho_2(t)$. Using the last (norm) equation and it's derivative, $\dot{\rho}_0 = -\dot{\rho}_2$, we finally obtain an equation solely for $\rho_2(t)$,

$$-\dot{\rho}_2 \sim \frac{1}{n^\tau} \left[1 - \frac{3}{2}(\theta + \rho_2)^{1-\tau} + \frac{1}{2}\rho_2^{1-\tau} \right], \quad (24)$$

or, using the fact that ρ_2 almost instantly takes on the value of $\rho_1(0) + \rho_2(0) - \theta = 1 - \theta - \rho_0(0)$ (see Fig. 5),

$$t \sim n^\tau \int_{\rho_2(t)}^{1-\theta-\rho_0(0)} \frac{2d\xi}{2 - 3(\theta + \xi)^{1-\tau} + \xi^{1-\tau}}. \quad (25)$$

We can estimate the duration of the jam, t_{jam} , by setting $\rho_2(t_{\text{jam}}) \approx 0$, see Fig. 5:

$$t_{\text{jam}} \sim n^\tau f_\tau(1 - \theta - \rho_0(0)), \quad (26)$$

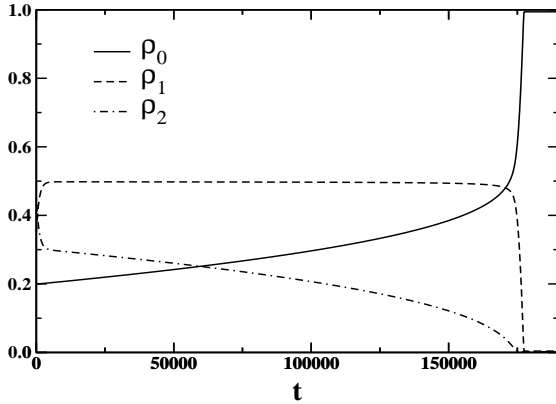


FIG. 5: Plot of the typical evolution of the system in Eqs. (18) for some generic initial condition that leads to a jam. Shown are $\rho_0(t)$ (red), $\rho_1(t)$ (yellow), and $\rho_2(t)$ (green) for $n = 1000$, $\tau = 2$, $\theta = 0.5$ and initial conditions $\rho_0(0) = 0.2$, $\rho_1(0) = 0.35$, and $\rho_2(0) = 0.45$. Since $\rho_1(0) < \theta$, ρ_1 fills up to θ almost instantly with variables from ρ_2 while ρ_0 stays constant. After that, $\rho_1 \approx \theta$ for a very long time ($\gg n$) while variables slowly move down through it. Eventually, after $t = O(n^\tau)$, ρ_2 vanishes and EO can empty out ρ_1 directly which leads to the ground state $\rho_0 = 1$ ($e = 0$) almost instantly.

where we defined

$$f_\tau(x) = \int_0^x \frac{2d\xi}{2 - 3(\theta + \xi)^{1-\tau} + \xi^{1-\tau}} \quad (x \geq 0). \quad (27)$$

Thus, the duration of the jam scales with n^τ times a constant that depends on τ , θ , and the initial conditions. As stated before, if the initial conditions keep $\rho_1(0) + \rho_2(0) < \theta$, most likely there will be no jam, reflected in the fact that $f_\tau(x)$ goes to zero for $x \rightarrow 0$. The asymptotic scaling in Eq. (26) conforms well with our numerical simulations: with $f_2(0.3) \approx 0.162$ and $n = 1000$ we obtain $t_{\text{max}} \approx 162\,000$, in good agreement with Fig. 5.

The long-lived jams that occur for $\tau > 1$ will have a significant effect on the outcome of a local search with EO, which proceeds merely with a finite runtime t_{max} . For instance, for $t_{\text{max}} = O(n)$ there are always some initial conditions for which the jam can not be resolved before t_{max} , resulting in $e > 0$. Thus, the τ -EO implementation faces two conflicting priorities: On one side, larger τ increase the quality of the steady-state result for e , away from the random-walk-like behavior at $\tau < 1$, see Fig. 4. On the other side, $\tau > 1$ increases the chance to get locked into a jam and never to reach that steady state in finite runtime, see Fig. 5. In between these conflicting interests, we find a preferred value for τ_{opt} that averts both, the jam and the random walk, such that $\langle e \rangle$, averaged over initial conditions, is minimized.

Let us assume we fix runtime to be $t_{\text{max}} = a n$, where a is a constant with $a \ll n$, so that $n < t_{\text{max}} \ll n^\tau$ for $\tau > 1$. If we had chosen $\tau < 1$ for our implementation, there are no jams but we are sure to obtain less than optimal results for $\langle e \rangle$ as in Fig. 4, so we will assume $\tau > 1$. In this case, we have to distinguish between three possible outcomes to a single run of the EO algorithm, depending on the initial conditions: (1) If $\rho_1(0) + \rho_2(0) < \theta$, the run will most certainly reach the optimal state, $e = 0$, within t_{max} updates, (2) even if $\rho_1(0) + \rho_2(0) > \theta$ but $t_{\text{max}} \gtrsim t_{\text{jam}}$ from Eq. (26), $e = 0$ may be reached. Only if (3) $\rho_1(0) + \rho_2(0) > \theta$ and $t_{\text{max}} \ll t_{\text{jam}}$ are satisfied, the search will get stuck in a state of $e > 0$, with a value that depends on the initial conditions. Averaging over all initial conditions, we find

$$\langle e \rangle \approx \frac{1}{\mathcal{N}} \int_0^1 d\rho_0 d\rho_1 d\rho_2 \delta(1 - \rho_0 - \rho_1 - \rho_2) \frac{1}{2} \left(\sum_{i=0}^2 i \rho_i \right) u(1 - \theta - \rho_0) u(f_\tau(1 - \theta - \rho_0)n^\tau - t_{\text{max}}), \quad (28)$$

where $u(x)$ is the Heaviside step-function and $\delta(x)$ is the Dirac delta-function. The norm is given by

$$\mathcal{N} = \int_0^1 d\rho_0 d\rho_1 d\rho_2 \delta(1 - \rho_0 - \rho_1 - \rho_2) = \frac{1}{2}. \quad (29)$$

Hence, we obtain

$$\langle e \rangle \approx \frac{3}{2} \int_0^{\max\{0, 1-\theta-f_\tau^{-1}(t_{\text{max}}/n^\tau)\}} d\rho_0 (1 - \rho_0)^2 \quad (30)$$

The average energy $\langle e \rangle$ in Eq. (30) will start to rise for increasing τ as soon as the upper integration limit becomes non-zero, or when $t_{\max} \approx f_{\tau}(1 - \theta)n^{\tau}$. If $t_{\max} \ll f_{\tau}(1 - \theta)n^{\tau}$, i. e. for $\tau \gg 1$, Eq. (30) predicts for the average energy $\langle e \rangle = (1 - \theta^3)/2$.

Since $\langle e \rangle$ will reach its minimum value right before the onset of jams cause its rise, we can use this relation to estimate the optimal value of τ . In effect, this justifies the connection between τ_{opt} and the “edge of ergodicity” noted in Ref. [13]. Since the dependence of f_{τ} on τ is much weaker than the exponential n^{τ} , we can write

$$\begin{aligned} \tau_{\text{opt}} &\sim \frac{\ln(t_{\max}/f_{\tau}(1 - \theta))}{\ln n}, \\ &\sim 1 + \frac{\ln(a/f_{\tau}(1 - \theta))}{\ln n}, \end{aligned} \quad (31)$$

where we have used our choice $t_{\max} = an$. In recognition of the fact that $\tau \rightarrow 1^+$ for $n \rightarrow \infty$, we can simplify the last expression by expanding $f_{\tau}(x)$ in that limit to get

$$f_{\tau}(x) \sim \frac{2}{\tau - 1} \int_0^x \frac{d\xi}{\ln \left[\frac{(\theta + \xi)^3}{\xi} \right]} \quad (\tau \rightarrow 1). \quad (32)$$

Note that the pole at $\tau = 1$ is a generic consequence of Eq. (9), independent of the choice of individual the $T_{i,j}$ depicted in Fig. 3c. If we insert Eq. (32) into Eq. (31), we *exactly* reproduce the n dependence given in Ref. [22], see Eq. (6) above. Numerical, we get at $\theta = 1/2$ for $f_{\tau}(1/2) \approx (2 \ln 2 - 1)/(\tau - 1)$, and using $a = 100$ and $n = 10, 100, 1000$, and 10000 , Eq. (31) predicts $\tau_{\text{opt}} \approx 3.5, 2.1, 1.6$, and 1.4 .

We can compare this prediction with numerical simulations of τ -EO applied directly to the jamming system described in Fig. 3c [not just the evolution equation in (18) that use averaged probabilities Q]. In Fig. 6 we show the results for $\langle e \rangle$ as a function of τ for $n = 10, 100, 1000$, and 10000 at $t_{\max} = 100n$. Initially, for $\tau \lesssim 1$, $\langle e \rangle$ reaches the steady state result from Fig. 4 for any initial condition. But, as predicted, $\langle e \rangle$ reaches a minimum at a τ_{opt} beyond which it starts to rapidly deviate from the steady state solution. This is the “ergodic edge” beyond which unresolved jams effect the observed value of $\langle e \rangle$. Our prediction for τ_{opt} appears to become increasingly accurate for $n \rightarrow \infty$. Furthermore, for $\tau \rightarrow \infty$, Eq. (30) predicts $\langle e \rangle \approx 0.44$ for $\theta = 1/2$, in good approximation to the numerical value seen in Fig. 6.

IV. CONCLUSION

We have presented a simple model to analyze the properties of local search heuristics. This model was applied to extremal optimization and we found conditions under which EO exhibited the same phenomenology on the model as it does on real combinatorial optimization

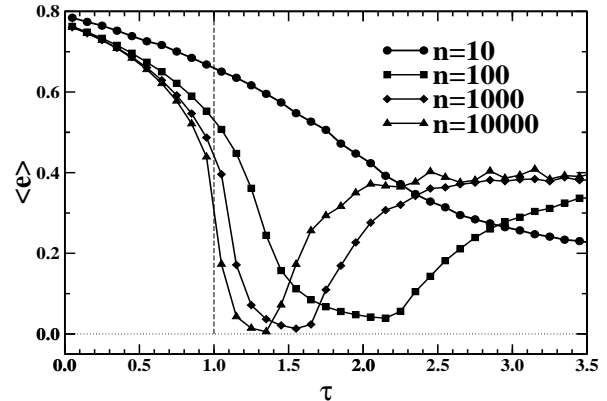


FIG. 6: Plot of the energy $\langle e \rangle$ averaged over many τ -EO runs with different initial conditions as a function of τ for $n = 10, 100, 1000$, and 10000 and $\theta = 1/2$. For small values of τ , $\langle e \rangle$ closely follows the steady state solutions plotted in Fig. 4. It reaches a minimum at a value near the prediction for $\tau_{\text{opt}} \approx 3.5, 2.1, 1.6$, and 1.4 , and rises sharply beyond that. It reaches an asymptotic value approaching the prediction of $\langle e \rangle \sim 7/16 \approx 0.44$ for $\tau \rightarrow \infty$.

problems as exemplified here by a frustrated spin system on a random graph. The analytical results from the model in Eq. (31) closely resemble the predictions from Refs. [13, 22] [see Eq. (6)].

Of course, the model is tailored more toward understanding the EO mechanism and does not represent all of the features of a hard optimization problem. [After all, it takes EO only $O(n^{\tau})$ updates to find the ground state in the worst case for the model.] Thus, finding a non-trivial value for τ_{opt} in the model merely provides an analogy. For instance, τ_{opt} is somewhat dependent on the relationship of t_{\max} to n . If $t_{\max} = O(n^l)$ then $\tau_{\text{opt}} \sim l - 1$ for $n \rightarrow \infty$ according to the model. In this regard the analogy seems to hold in every respect for the graph bipartitioning problem in Refs. [13, 22] where $t_{\max} \sim n$. But in our numerical simulations for spin glass systems in Sec. II displayed in Fig. 2, or in Ref. [5], typically $O(n^{3-4})$ updates were required to obtain consistent results for increasing n , still, $\tau_{\text{opt}} \rightarrow 1^+$ was found.

We believe that our observation for the behavior of EO is quite robust under variation of the entries for \mathbf{T} . More complicated choices for \mathbf{T} (which may be analytically less tractable) could be made to represent hard problems more closely. In this sense, the separation between \mathbf{T} and \mathbf{Q} allows to study comparisons between different update modes, and even with other local search procedures. As our examples in Figs. 3a-c show, simple choices of \mathbf{T} can lead to interesting scenarios, although it is always an annealed approximation. For instance, one could analyze the properties of EO for different choices of the probability distribution over the ranks in Eqs. (5,16).

It is more difficult to construct the Q 's for simulated annealing. Let's assume that we consider a variable in state j for an update. Certainly, Q_j would be proportional to ρ_j , since variables are randomly selected for an update. The Boltzmann factor $e^{-\beta\Delta E_j}$ for the potential update of a variable in j , aside from the inverse temperature $\beta(t)$, only depends on the entries for $T_{i,j}$:

$$\begin{aligned}\Delta E_j &= n\Delta e_j, \\ &= \frac{n}{2} \left[\sum_i i\rho_i(t+1) - \sum_i i\rho_i(t) \right]_j, \\ &= \frac{n}{2} \sum_i iT_{i,j},\end{aligned}\quad (33)$$

where the subscript j expresses the assumption that a variable in state j is considered for an update. Hence, we find for the average probability of an update of a variable in state j

$$Q_j \propto \rho_j \min \left\{ 1, \exp \left[-\beta \sum_i iT_{i,j} \right] \right\}, \quad (34)$$

which is still short of a proper normalization. Similarly, comparisons with other methods such as threshold annealing [33] can be considered.

ACKNOWLEDGMENTS

We would like to acknowledge helpful discussions with participants of the 2001 Telluride workshop on energy landscapes, in particular Allon Percus and Paolo Sibani. Special thanks to Remi Monasson whose visit to Emory inspired the idea.

REFERENCES

[†] Electronic address: sboettc@emory.edu

[‡] Electronic address: mic@mathcs.emory.edu

- [1] M. R. Garey and D. S. Johnson, *Computers and Intractability, A Guide to the Theory of NP-Completeness* (W. H. Freeman, New York, 1979).
- [2] K. F. Pal, *Physica A* **223**, 283-292 (1996), and **233**, 60-66 (1996).
- [3] A. K. Hartmann, *Phys. Rev. B* **59**, 3617-3623 (1999), and *Phys. Rev. E* **60**, 5135-5138 (1999).
- [4] M. Palassini and A. P. Young, *Phys. Rev. Lett.* **85**, 3017 (2000).
- [5] S. Boettcher and A. G. Percus, *Phys. Rev. Lett.* **86**, 5211-5214 (2001).
- [6] K. K. Bhattacharya and J. P. Sethna, *Phys. Rev. E* **57**, 2553 (1998).
- [7] E. Tuzel and A. Erzan, *Phys. Rev. E* **61**, R1040 (2000).
- [8] R. G. Palmer and J. Adler, *Int. J. Mod. Phys. C* **10**, 667 (1999).
- [9] C. Desimone, M. Diehl, M. Jünger, P. Mutzel, G. Reinelt, G. Rinaldi, *J. Stat. Phys.* **80**, 487-496 (1995).
- [10] *Modern Heuristic Search Methods*, Eds. V. J. Rayward-Smith, I. H. Osman, and C. R. Reeves (Wiley, New York, 1996).
- [11] S. Kirkpatrick, C. D. Gelatt, and M. P. Vecchi, *Science* **220**, 671-680 (1983).
- [12] J. Holland, *Adaptation in Natural and Artificial Systems* (University of Michigan Press, Ann Arbor, 1975).
- [13] S. Boettcher and A. G. Percus, *Artificial Intelligence* **119**, 275-286 (2000).
- [14] S. Boettcher and A. G. Percus, in *GECCO-99: Proceedings of the Genetic and Evolutionary Computation Conference* (Morgan Kaufmann, San Francisco, 1999), 825-832.
- [15] S. Boettcher, M. Grigni, G. Istrate, and A. G. Percus, *Phase Transitions and Computational Complexity*, in preparation.
- [16] S. Boettcher, *J. Math. Phys. A* **32**, 5201-5211 (1999).
- [17] J. Dall and P. Sibani *cond-mat/0107475*.
- [18] P. Cheeseman, B. Kanefsky, and W. M. Taylor, in *Proc. of IJCAI-91*, eds. J. Mylopoulos and R. Rediter (Morgan Kaufmann, San Mateo, CA, 1991), pp. 331-337.
- [19] See *Frontiers in problem solving: Phase transitions and complexity*, Special issue of *Artificial Intelligence* **81**:1-2 (1996).
- [20] R. Monasson, R. Zecchina, S. Kirkpatrick, B. Selman, and L. Troyansky, *Nature* **400**, 133-137 (1999), and *Random Struct. Alg.* **15**, 414-435 (1999).
- [21] S. Cocco and R. Monasson, *Phys. Rev. Lett.* **86**, 1654-1657 (2001), and *Phys. Rev. E* (to appear).
- [22] S. Boettcher and A. G. Percus, *Phys. Rev. E* **64**, 026114 (2001).
- [23] L. Viana and A. J. Bray, *J. Phys. C* **18**, 3037 (1985).
- [24] K. Y. M. Wong and D. Sherrington, *J. Phys. A: Math. Gen* **20**, L793 (1987);
- [25] M. Mezard and G. Parisi, *Europhys. Lett.* **3**, 1067 (1987).
- [26] J. R. Banavar, D. Sherrington, and N. Sourlas, *J. Phys. A: Math. Gen* **20**, L1 (1987).
- [27] B. Bollobas, *Random Graphs*, (Academic Press, London, 1985).
- [28] H. M. Jaeger, S. R. Nagel, R. P. Behringer, *Rev. Mod. Phys* **68** 1259-1273 (1996).
- [29] E. Ben-Naim, J. B. Knight, E. R. Nowak, H. M. Jaeger, and S. R. Nagel, *Physica D* **123**, 380-385 (1998).
- [30] F. Ritort, *Phys. Rev. Lett.* **75**, 1190-1193 (1995).
- [31] Actually, for $\theta \leq 0.385$, there is a transition to having three solutions near $\tau = 1$, resulting in a first-order transition for $n \rightarrow \infty$. We will only discuss

$\theta > 0.385$ here.

- [32] R. G. Palmer, D. L. Stein, E. Abrahams, and P. W. Anderson, Phys. Rev. Lett. **53**, 958 (1984).
- [33] A. Franz, K.-H. Hoffmann, P. Salamon, Phys. Rev. Lett. **86** 5219-5222 (2001).